JOURNAL OF AIRCRAFT
Vol. 46, No. 2, March–April 2009

Aeroship: A Hybrid Flight Platform

Tianshu Liu,* W. W. Liou,† and M. Schulte‡
Western Michigan University, Kalamazoo, Michigan 49008

DOI: 10.2514/1.39950

This paper describes the simplest hybrid configuration, called an aeroship, that integrates an airship module and a wing to meet demanding requirements in takeoff/landing, low-speed flight, and control/maneuver for certain challenging flight missions. A flight performance analysis of an aeroship is given, particularly on the optimum ratio between the aerostatic lift and the total weight to achieve the maximum lift-to-drag ratio. To critically examine the conceptual design and performance analysis, a remote-controllable model aeroship is built and tested in flight. The results obtained by using a stereo-videogrammetric system in flight testing are consistent with the performance analysis.

I. Introduction

THE idea of using a combination of aerostatic and aerodynamic forces, such as with a winged airship and a lifting-body airship, has been proposed [1–4]. The impetus for this development of a hybrid air vehicle called an *aeroship* originates from the need for air vehicles for personal flight, planetary flight, and high-altitude flight that present formidable technical challenges to conventional flight platforms. The idea of personal flying machines such as flying cars seems to be as old as aviation itself, yet it continues to attract considerable attention. Personal air vehicles require some stringent features in takeoff/landing, low-speed maneuverability and controllability, piloting, and environmental impact [5]. The existing designs of air vehicles cannot meet most of the necessary requirements for personal flight. Unmanned planetary flight (e.g., Mars flight) and high-altitude (near-space) flight at low speeds also pose unique challenges. Several previously proposed concepts such as fixed-wing aircraft [6–9], rotorcraft [10–14], flapping flyers [15,16], and balloons [17] have serious problems in short takeoff/landing, low-speed maneuverability, and long endurance in rarefied atmospheres.

No single conventional flight platform can provide a satisfactory, feasible, and economical solution to personal flight, planetary flight, and high-altitude flight. Therefore, a hybrid platform that integrates an airship and a wing into a single system seems feasible to achieve the optimal performance in takeoff/landing, control, and maneuver in low-speed flight [18]. This paper describes an aeroship that is the simplest integration of a conventional airship module and a straight wing. A flight performance analysis for the aeroship is presented. To validate the conceptual design and performance analysis, a remote-controllable model aeroship is designed, built, and tested in flight. The flight-testing results are compared with the performance analysis.

Presented as Paper 3922 at the 24th AIAA Applied Aerodynamics Conference, San Francisco, CA, 5–8 June 2008; received 22 July 2008; revision received 20 October 2008; accepted for publication 8 November 2008.

*Associate Professor, Department of Mechanical and Aeronautical Engineering, Parkview Campus; tianshu.liu@wmich.edu. Senior Member AIAA.

†Professor, Department of Mechanical and Aeronautical Engineering, Parkview Campus; william.liou@wmich.edu. Associate Fellow AIAA.

‡Graduate Student, Department of Mechanical and Aeronautical Engineering, Parkview Campus. Student Member AIAA.

II. Concept

The aeroship platform consists of a suitably sized airship module and a wing/propulsion module. The total weight W of an aeroship is partially supported by the aerostatic lift L_{ship} from the airship module, and the remaining weight $\Delta W = W - L_{\text{ship}}$ is supported by the aerodynamic lift L_{wing} from the wing/propulsion module. The effective weight ΔW is an important factor in the performance of an aeroship, providing a natural downward force for landing and maneuver during flight. Figure 1 illustrates the simplest aeroship configuration driven by propellers for personal flight and unmanned high-altitude flight. For this configuration, a conventional axisymmetrical streamlined hull is directly adopted for the airship module [18], and a straight wing is installed beneath the hull at a sufficient distance. This configuration is not only structurally simple, but also feasible for a preliminary aerodynamic analysis in which complicated aerodynamic interference between the airship module and the wing/propulsion module is neglected as a second-order effect.

The relevant parameters are introduced here. In a first-order analysis in which the aerodynamic interaction between the airship module and wing/propulsion module is sufficiently weak, the lift and drag of the two modules can be considered independently in a preliminary analysis. The buoyancy lift generated by the airship module is given by

$$L_{\text{ship}} = g(\rho - \rho_g)V_{\text{ship}}$$

where V_{ship} is the airship volume, and ρ and ρ_g are the gas densities outside and inside the airship, respectively. For example, in the earth atmosphere, ρ and ρ_g are the densities of air and a lifting gas such as helium. Here, the buoyancy lift coefficient is defined as

$$C_{L_{\text{ship}}} = L_{\text{ship}}/g\rho V_{\text{ship}} = 1 - \rho_g/\rho$$

The drag coefficient for the airship is conventionally defined as

$$C_{D_{\text{ship}}} = D_{\text{ship}}/(\rho U^2 S_{\text{ship}}/2)$$

where S_{ship} is the characteristic area of the airship module, and U is the flight speed. The volume V_{ship} is generally related to the area S_{ship} by

$$V_{\text{ship}} = a_{\text{ship}}(S_{\text{ship}})^{3/2}$$

where a_{ship} is a factor depending on the airship geometry. In some literature, S_{ship} is defined as the frontal (or front-projected) area of airship, and it is sometimes defined as $S_{\text{ship}} = V_{\text{ship}}^{2/3}$. The conventional definitions of the lift and drag coefficients are used for the wing: that is,

$$C_{L_{\text{wing}}} = L_{\text{wing}}/(\rho U^2 S_{\text{wing}}/2), \qquad C_{D_{\text{wing}}} = D_{\text{wing}}/(\rho U^2 S_{\text{wing}}/2)$$

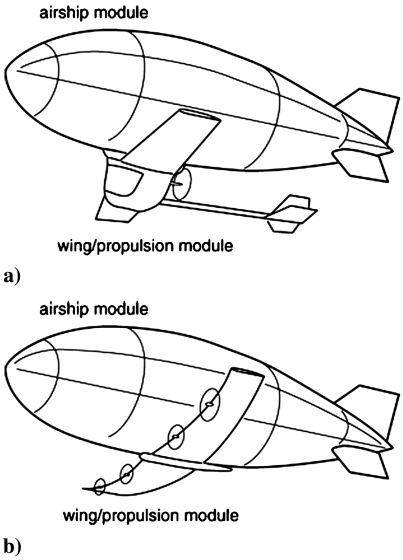

Fig. 1 Basic aeroship configurations for a) personal flight and b) unmanned high-altitude flight.

where D_{wing} includes both the parasite drag and induced drag of the wing.

The total lift and drag of an aeroship are, respectively,

$$L = C_{L_{\text{ship}}} g\rho V_{\text{ship}} + C_{L_{\text{wing}}}(\rho U^2 S_{\text{wing}}/2) \tag{1}$$

$$D = C_{D_{\text{ship}}}(\rho U^2 S_{\text{ship}}/2) + C_{D_{\text{wing}}}(\rho U^2 S_{\text{wing}}/2) \tag{2}$$

The total drag coefficient of an aeroship can be defined as

$$C_D = D/(\rho U^2 S_{\text{wing}}/2) = C_{D_{\text{ship}}} R_S + C_{D_{\text{wing}}} \tag{3}$$

where $R_S = S_{\text{ship}}/S_{\text{wing}}$ is the ratio between the characteristics areas of the airship and wing modules. Further, the total drag coefficient can be written as

$$C_D = C_{D,0} + KC_{L_{\text{wing}}}^2$$

where the total parasite (zero-lift) drag of an aeroship

$$C_{D,0} = C_{D_{\text{ship}}} R_S + C_{D_{\text{wing}},0}$$

is the sum of the airship module drag and wing parasite drag. The factor $K = (\pi e \text{AR})^{-1}$ is related to the wing induced drag, where e is the span efficiency, and AR is the wing aspect ratio. Care should be taken when defining the total-lift coefficient, because there is a mixture of the two distinct mechanisms for generating lift. In fast forward flight, the total lift coefficient of an aeroship is defined as

$$C_L = L/(\rho U^2 S_{\text{wing}}/2) = C_{L_{\text{ship}}} R_F + C_{L_{\text{wing}}}$$

where the parameter

$$R_F = gV_{\text{ship}}/(U^2 S_{\text{wing}}/2)$$

describes a balance between the buoyancy force and the aerodynamic force. The total lift-to-drag ratio of an aeroship is

$$L/D = (C_{L_{\text{ship}}} R_F + C_{L_{\text{wing}}})/(C_{D_{\text{ship}}} R_S + C_{D_{\text{wing}}})$$

III. Optimum Ratio Between Buoyancy Lift and Weight at Maximum L/D

The performance analysis for the aeroship is parallel to that for aircraft, as described in the Appendix [19]. Figure 2 shows the diagrams of force balance on aeroship. In contrast to aircraft, the effective weight ΔW of an aeroship, rather than the total weight W, plays a key role in the performance analysis. Here, the maximum lift-to-drag ratio L/D and the corresponding optimum ratio between the buoyancy lift and the total weight are sought, which are useful for the design of an aeroship. In general, the lift-to-drag ratio is

$$\frac{C_L}{C_D} = \frac{L}{D} = \frac{C_L}{C_{D,0} + K(C_L - R_F C_{L_{\text{ship}}})^2} \tag{4}$$

For the maximum L/D, differentiating Eq. (4) with respect to C_L and then setting the result equal to zero, we have

$$C_L = \sqrt{C_{D,0}/K + R_F^2 C_{L_{\text{ship}}}^2} \tag{5}$$

Substitution of Eq. (5) into Eq. (4) yields

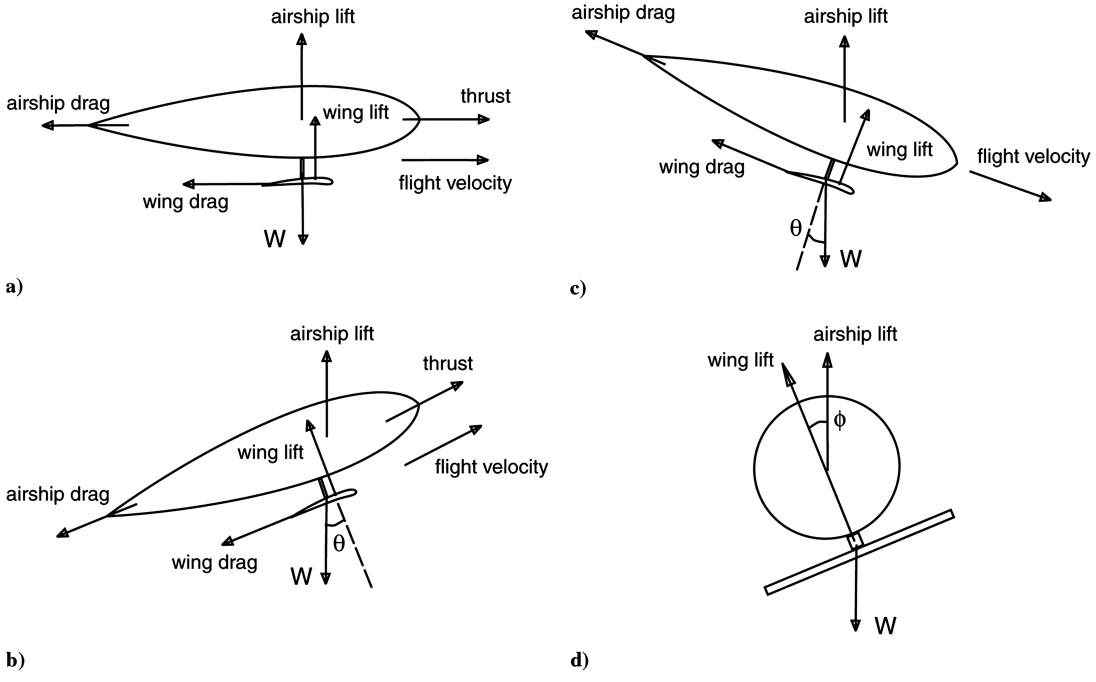

Fig. 2 Diagrams of force equilibrium on aeroship for a) level steady flight, b) climbing, c) gliding, and d) level turn.

$$\left(\frac{L}{D}\right)_{\max} = \frac{\sqrt{C_{D,0}/K + R_F^2 C_{L_{\text{ship}}}^2}}{C_{D,0} + K(\sqrt{C_{D,0}/K - R_F^2 C_{L_{\text{ship}}}^2} - R_F C_{L_{\text{ship}}})^2} \tag{6}$$

Equation (6) can be expressed by

$$(L/D)_{\max} = K^{-1} f(R_F C_{L_{\text{ship}}}, C_{D,0}/K) \tag{7}$$

where the function $f(x, p)$ is defined as

$$f(x, p) = \frac{\sqrt{p + x^2}}{p + (\sqrt{p - x^2} - x)^2} \tag{8}$$

The function $f(x, p)$ has a maximum point in $x \in [0, \sqrt{p}]$. For a given $C_{D,0}/K$, $(L/D)_{\max}$ can be further maximized by differentiating Eq. (7) with respect to $R_F C_{L_{\text{ship}}}$. Because a closed-form solution cannot be obtained, the twice-maximized value $(L/D)_{\max 2}$ is found by a standard numerical scheme for optimization. The optimum value of $R_F C_{L_{\text{ship}}}$ is found as a function of $C_{D,0}/K$ over a certain range, and a regression to fit the numerical data is

$$(R_F C_{L_{\text{ship}}})_{\text{op}} = 0.761\sqrt{C_{D,0}/K} \tag{9}$$

Substitution of Eq. (9) into Eq. (7) yields

$$(L/D)_{\max 2} = 1.241/\sqrt{C_{D,0}K} \tag{10}$$

Compared with a classical relation

$$(L/D)_{\max} = 0.5/\sqrt{C_{D_{\text{wing}},0}K}$$

for aircraft, the achievable maximum L/D for the aeroship is

$$\frac{(L/D)_{\max 2,\ \text{aeroship}}}{(L/D)_{\max,\ \text{aircraft}}} = \frac{2.482}{\sqrt{1 + R_S C_{D_{\text{ship}}}/C_{D_{\text{wing},0}}}} \tag{11}$$

For $R_S C_{D_{\text{ship}}}/C_{D_{\text{wing},0}} < 5.16$, the aeroship has a higher L/D than that for aircraft. Similarly, substitution of Eq. (9) into Eq. (5) leads to

$$C_L = 1.257\sqrt{C_{D,0}/K} \tag{12}$$

A comparative relation for C_L at the maximum L/D is

$$\frac{(C_L)_{\text{aeroship}}}{(C_L)_{\text{aircraft}}} = 1.257\sqrt{1 + R_S C_{D_{\text{ship}}}/C_{D_{\text{wing},0}}} \tag{13}$$

Substitution of Eq. (12) into $W = L = \rho U^2 S_{\text{wing}} C_L/2$ yields an expression for the velocity at $(L/D)_{\max}$:

$$U_{(L/D)_{\max}} = 0.891\left(\frac{2}{\rho}\sqrt{\frac{K}{C_{D,0}}}\frac{W}{S_{\text{wing}}}\right)^{1/2} \tag{14}$$

Accordingly, a comparative relation with respect to aircraft is

$$\frac{U_{(L/D)\ \max,\ \text{aeroship}}}{U_{(L/D)\ \max,\ \text{aircraft}}} = \frac{0.891}{\sqrt{1 + R_S C_{D_{\text{ship}}}/C_{D_{\text{wing},0}}}} \tag{15}$$

As indicated by Eqs. (13) and (15), the aeroship at the maximum L/D has a larger lift coefficient, but a lower velocity, than with aircraft. Furthermore, as a consequence of a constraint imposed by the optimality condition equation (9) for $(L/D)_{\max 2}$, substitution of Eq. (14) into Eq. (9) gives an optimum ratio between the buoyancy lift and the total weight of an aeroship:

$$(L_{\text{ship}}/W)_{(L/D)_{\max}} = 0.6041 \tag{16}$$

This is a useful relation for the preliminary design of an aeroship. For a given airship weight, the airship module volume V_{ship} can be further estimated by using Eq. (16) to achieve the maximum L/D.

IV. Flight Testing of the Model Aeroship

A. Design

To validate the proposed concept and the performance analysis, a remote-controllable model aeroship was designed and built for flight testing [20]. Figure 3 shows the model aeroship on the ground and in flight testing. Table 1 lists the design parameters of the components of the model aeroship. The total weight of the model aeroship was 19 N. The airship module was a commercially available blimp or gas envelope with a maximum length of 2.3 m and a maximum diameter of 1.1 m. A suitable airframe module was built in-house to fit with the gas envelope.

In flight tests, the blimp supported 60% of the total weight of the model aeroship, which is the optimum value given by the performance analysis. Three fins made of 6-mm-thick Depron foam were installed on the left, right, and top sides at the rear of the gas envelope for required stability and control. The fin size was 0.46 m at the root, tapered to 0.3 m at the tip, with a 0.33 m span. The leading edge was swept at an angle of 25 deg. The straight wing had a span of 1.52 m and a chord of 0.203 m, and the wing section was the NACA4312 airfoil section.

All structural components of the wing and tails were constructed using balsa ribs and spars covered with thin white MonoKote sheets. A fiberglass beam was used as a main frame on which all of the components were attached, including the blimp, motor, with a

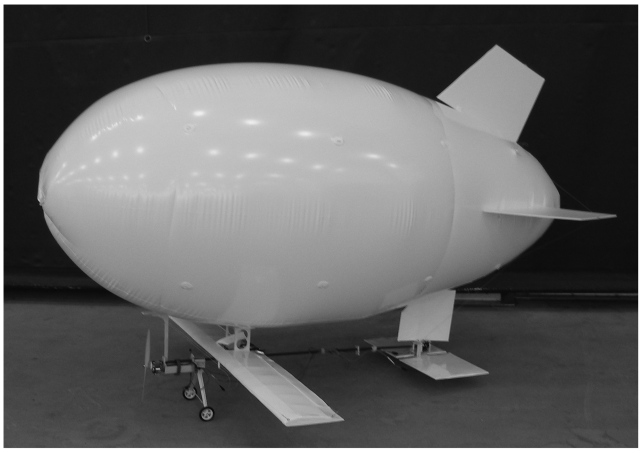

a)

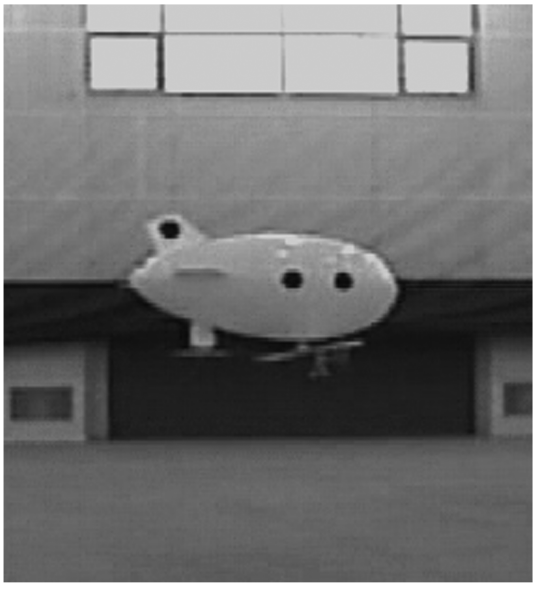

b)

Fig. 3 Remote-controllable model aeroship a) on the ground and b) in flight testing.

Table 1 Design parameters for the model aeroship

Parameters	Values
Total weight W, N	19
Gas envelope	
Volume, m^3	1.08
Gross buoyancy lift, N	13.3, 70% W
Weight of envelope, kg	0.48
Front-projected area, m^2	0.98
Vertical-projected area, m^2	1.5
Maximum length, m	2.3
Maximum diameter, m	1.1
Horizontal fin area, m^2	0.25
Vertical fin area, m^2	0.126
Wing parameters	
Wing section	NACA4312
Span, M	1.52
Chord, M	0.203
Wing area, m^2	0.309
Vertical tail parameters	
Cross section	Flat plate
Area, m^2	0.053
Rudder area, m^2	0.053
Vertical tail volume	0.102
Horizontal tail parameters	
Cross section	Flat plate
Area, m^2	0.155
Elevator area, m^2	0.155
Horizontal tail volume	2.09

gearbox connecting a propeller, batteries, servos, wing, and tails. The Hitec model HS-65HB servos were used for actuating the tails, which were capable of delivering torque of 0.19 N · m and weighed only 11 g. An electric motor (JustGoFly model 450TH) was chosen as the power source for the model aeroship, which was capable of producing up to 300 W of power. To keep the motor cool and within safety limits, the motor was only run below 200 W. A propeller of a 12 in. diameter with an 8 deg pitch was used in geared drive mode, which was able to provide more than 18 N of thrust. A three-cell lithium polymer battery pack was chosen for the power supply, which had a higher energy density than many other commercial batteries.

B. Flight Testing

Fight tests were conducted in the indoor tennis court at Western Michigan University. To accurately determine the flight performance of the model aeroship, a two-camera videogrammetric system was used to measure the three-dimensional (3-D) coordinates of three black targets on the aeroship during flight at a rate of 15 frames per second. The focal length of the camera was 8 mm. Figure 4 illustrates the two-camera system viewing the targets on the model aeroship. Before tests, the camera system was calibrated to determine the exterior and interior orientation parameters of the cameras based on a known target field in a designated ground coordinate system [21].

For such a large measurement volume, a known target field was established by sequentially placing a pole with two targets that were, respectively, at 1 and 2 m in height from the ground at 5 known ground locations. The volume of the target field was 6 m in width, 15 m in depth, and 2 m in height. The targets on it at these locations were imaged by cameras. Thus, a 3-D target field and the corresponding image coordinates were reconstructed by combining these images. Camera calibration was done by using an optimization method [22]. The calibration error in the image plane was about 0.008 mm, which was a relatively large error in such videogrammetric measurements. When a target was placed at 20 m away from a camera with an 8 mm focal length, this error would lead to an error of 20 mm in the object space. A general uncertainty analysis of videogrammetric measurements in aerodynamic testing was given by Burner et al. [23].

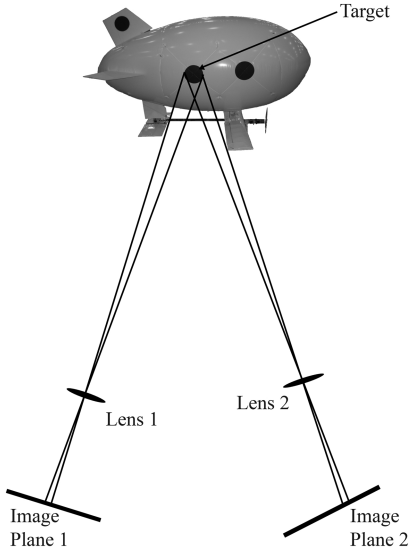

Fig. 4 Illustration of stereo-videogrammetric measurements of an aeroship flight.

The 3-D coordinates of the targets in the object space were calculated by photogrammetric intersection from a time sequence of image pairs recorded in flight. Then, from the 3-D coordinates of the three targets, the position and attitude of the model aeroship in flight were determined as a function of time. The data measured in flight testing were compared with the performance analysis for the model aeroship in Sec. III and the Appendix. Table 2 compares the estimated and measured performance data for the model aeroship. It is found that the first-order simplified performance analysis gives consistent results with the measurements.

C. Flight Performance

The takeoff performance of the model aeroship was examined. Figure 5 shows the rate of climb, speed, and position of the model aeroship in takeoff. From Fig. 5, it can be seen that the takeoff distance for the model aeroship was approximately 3 m and the velocity at the time of takeoff was approximately 4.2 m/s. These results are consistent with the estimated data given by the performance analysis, as shown in Table 2. Because the power for takeoff was significantly higher than that for cruising in flight tests, the estimated 100% increased power was used in the takeoff analysis. It should be noted that the measured takeoff data shown here was taken from a normal takeoff. The pilot was actually able to perform the takeoff maneuver in a much shorter distance.

The next maneuver measured using stereo videogrammetry was the landing of the model aeroship. Figure 6 shows the landing position, the descent rate (negative rate of climb), and the landing velocity. The model aeroship had a descent rate of about 1 m/s before touchdown. At approximately 3.5 m, the aeroship began to have a positive vertical velocity, reflecting a bounce right after

Table 2 Estimated and measured performance parameters for model aeroship

Parameter	Estimated	Measured in flight
Takeoff ground roll	5 m	3 m
Takeoff speed	4.6 m/s	4.2 m/s
Approach angle in landing	15 deg	16.7 deg
Touchdown speed in landing	4.6 m/s	3.3 m/s
Maximum R/C	3.1 m/s	2.5 m/s
Angle at maximum R/C	30 deg	32.3 deg
Velocity at maximum R/C	6.1 m/s	4.5 m/s
Descent rate in glide	2.3 m/s	1.4 m/s
Glide angle	15.4 deg	19.4 deg
Stall speed	4.2 m/s	4.2 m/s
Minimum level-turn radius	5.5 m	3.6 m, (left), 5.3 m (right)

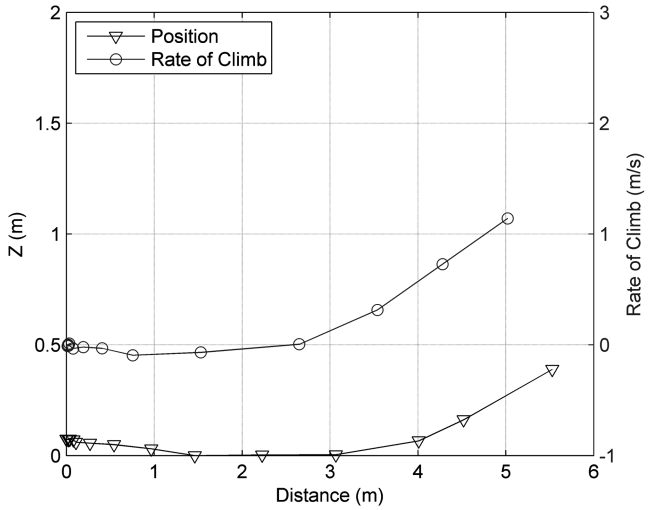

a)

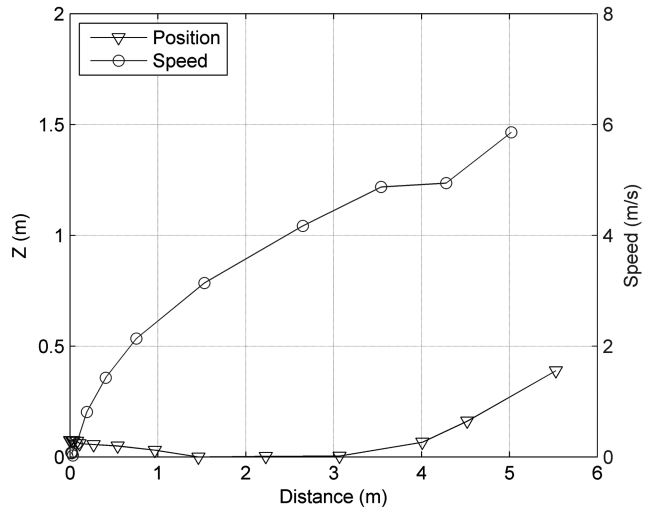

b)

Fig. 5 Takeoff: a) rate of climb and b) speed of the model aeroship in takeoff.

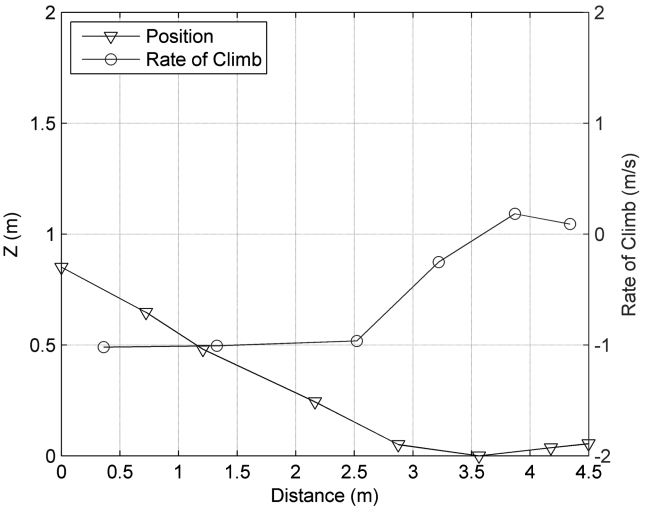

a)

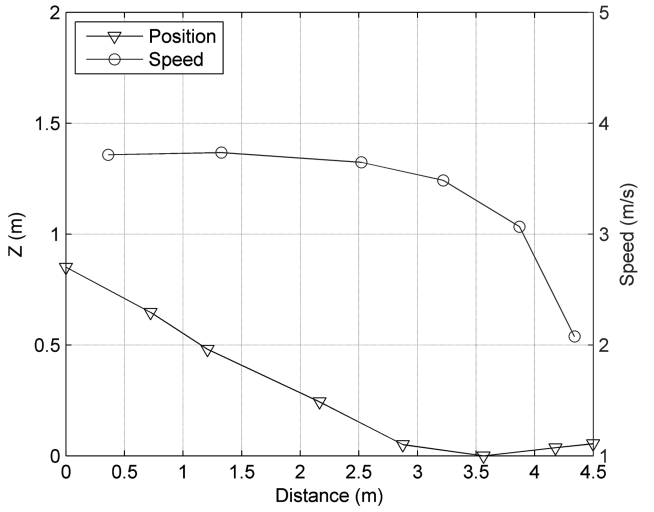

b)

Fig. 6 Landing: a) rate of climb decent rate and b) speed of the model aeroship in landing.

touchdown. The touchdown speed in landing was approximately 3.3 m/s, and the approach angle was 16.7 deg, which are consistent with the analysis for landing.

The short-climb maneuver was also used to test the performance of the model aeroship. Figure 7 shows the rate of climb, position, and speed of the model aeroship in the short climb. The test was conducted indoors, and therefore the climb maneuver had to be stopped before the aeroship hit the ceiling. The model aeroship climbed at an angle of 32.3 deg and reached the maximum rate of 2.5 m/s, consistent with the maximum climb rate and the corresponding climb angle given by the performance analysis. Although the short climb was not truly a steady climb, the test indicated that there seemed to be no problem maintaining the maximum climb rate if the ceiling was not present. During the test, the velocity of the aeroship started out relatively slow and rose sharply to 4.5 m/s.

In addition to the good climb performance, the aeroship design is well suited for glide. This is because the aerostatic lift is always present, and the buoyancy force created by the gas envelope tends to stabilize the craft and keep it upright and nearly level. Figure 8 shows the descent rate, position, and speed of the aeroship during power-off glide. This test was conducted over 2.6 s and the aeroship lost approximately 3 m of altitude. The descent rate was 1.4 m/s and the glide angle was 19.4 deg. Again, these measured results were consistent with those given by the analysis.

To test the turning performance, the pilot was instructed to fly level turns in both the left and right directions. During the test, the model aeroship rose no more than 1 m. Figure 9 shows the trajectory of the model aeroship in the horizontal plane (viewed from the top) during a left turn. The measured positional data were incomplete because a camera could not see the targets when the symmetrical axis of the aeroship was approximately parallel to the camera's optical axis. Therefore, to determine the turn radius, a circle was used to fit the available data as shown in Fig. 9. It is found that the turn radius was 3.6 m for the left turn. However, a similar fit for the right turn gave the turn radius of 5.3 m. Interestingly, the analysis gave the minimum turn radius of 5.5 m. The smaller left-turn radius could be caused by the torque generated by the motor and propeller, which was favorable to a left-turn maneuver. Tests were also conducted to determine the stall speed. The pilot was instructed to fly as slowly as possible without losing altitude. It was found that the stall speed for the model aeroship was 4.2 m/s, which was in agreement the estimated value.

V. Conclusions

The simplest hybrid flight platform, called an aeroship, is a direct integration of a conventional airship module and a wing/propulsion module. Such a simple configuration allows the first-order analysis of flight performance in which the aerodynamic interference between the two modules can be neglected. The maximum lift-to-drag ratio L/D can be achieved when 60% of the total weight is supported by

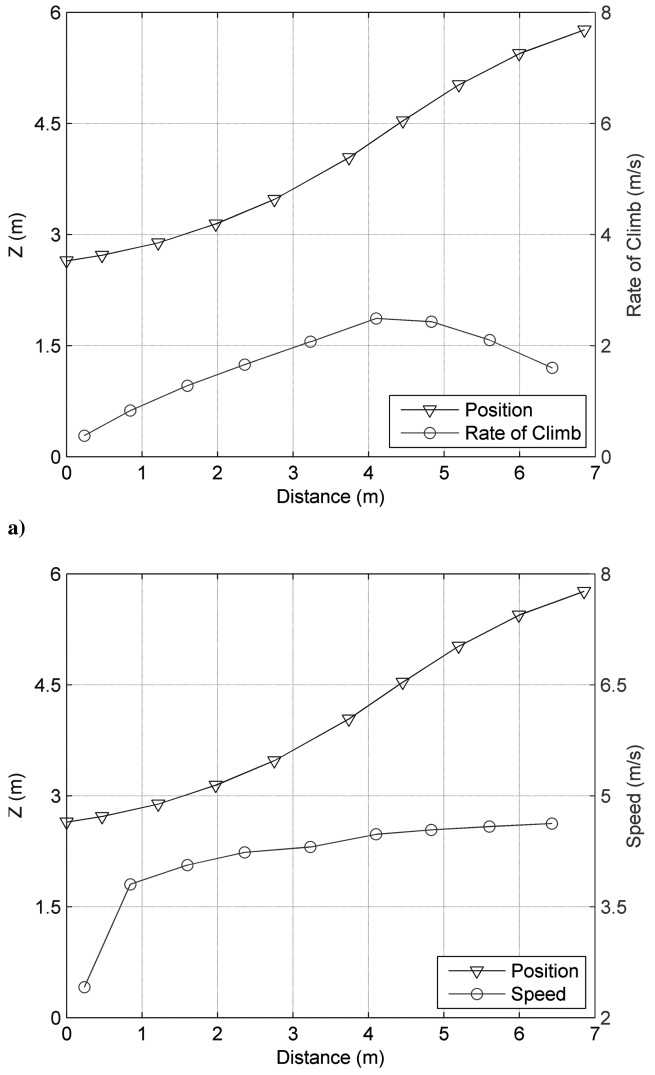

Fig. 7 Short climb of the model aeroship: a) rate of climb and b) speed.

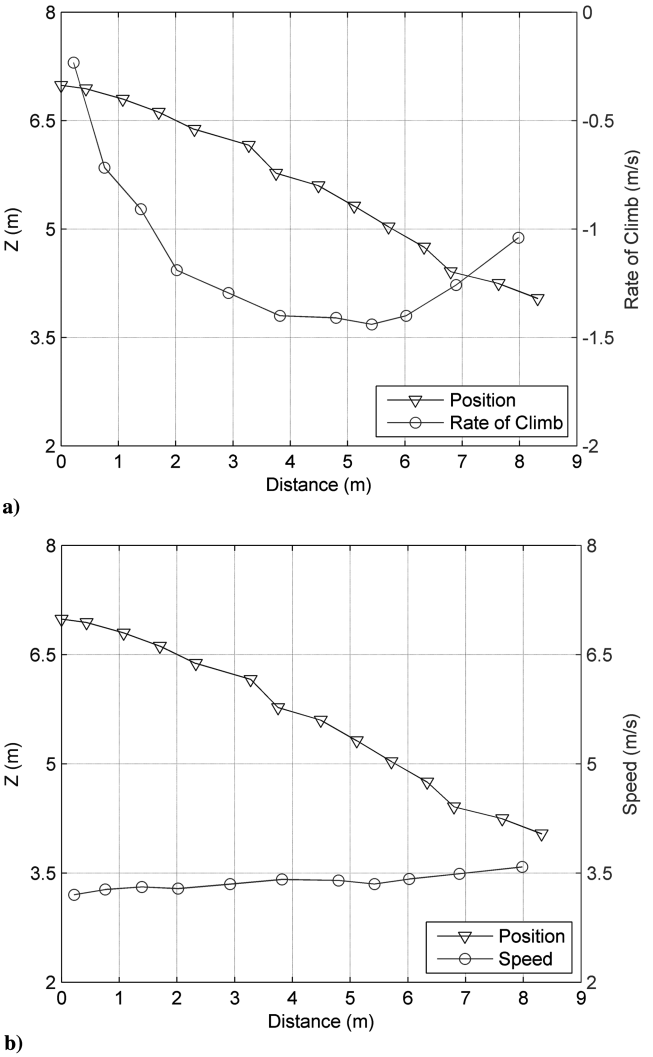

Fig. 8 Glide of the model aeroship: a) descent rate and b) speed.

the aerostatic lift. It is indicated that an aeroship offers some advantages over traditional flight platforms in challenging flight missions. Compared with aircraft, the aeroship has a larger maximum L/D, lower engine power required for cruise flight, lower cruising speed and stall speed, larger rate and angle of climb, smaller level-turn radius and speed, and shorter takeoff and landing ground rolls. A remote-controllable model aeroship is designed and built for flight testing. The flight trajectory and attitude of the model aeroship are measured by using stereo videogrammetry. The flight performance parameters measured in flight testing are consistent with the performance analysis, validating the concept of an aeroship.

Appendix: Performance Analysis of an Aeroship

I. Thrust Required for Level Flight

The analysis of the flight performance of an aeroship is parallel to the classical analysis of the aircraft performance [19]. As shown in Fig. 2a, because the total drag and effective weight $\Delta W = W - L_{\text{ship}}$ of an aeroship in steady level flight is balanced by the thrust T and the wing aerodynamic lift L_{wing}, respectively, the thrust required can be described by

$$T_R = D = \left(\frac{\rho U^2 S_{\text{wing}}}{2}\right)\left(C_{D_{\text{ship}}} R_S + C_{D_{\text{wing}},0}\right) + \frac{2KS_{\text{wing}}}{\rho U^2}\left(\frac{\Delta W}{S_{\text{wing}}}\right)^2 \tag{A1}$$

where $C_{D_{\text{wing}},0}$ is the wing parasite drag and the second term on the right-hand side is the induced drag of the wing. Just as with aircraft, a typical thrust-velocity curve given by Eq. (A1) for the aeroship is U-shaped, which has a minimum point for the thrust required. Compared with aircraft, however, the branch of the U-shaped curve

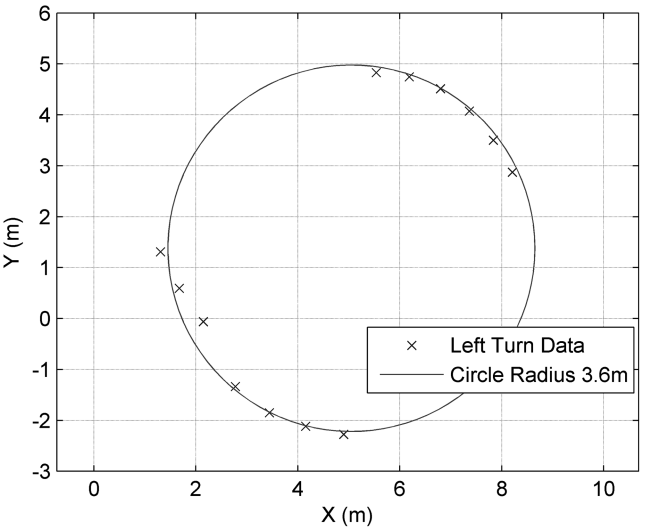

Fig. 9 Left level-turn position and projected turn circle of the model aeroship.

for the aeroship at higher speeds rises more rapidly as the speed increases, due to the larger parasite drag, whereas the branch at lower speeds decays more slowly, due to the smaller effective weight.

By solving Eq. (A1) for the velocity, a flight velocity is obtained that depends on the effective wing loading $\Delta W/S_{\text{wing}}$, the effective thrust-to-weight ratio $T_R/\Delta W$, and the total parasite drag $C_{D,0}$. At the minimum point of T_R, there is only one solution for the velocity under the optimality condition

$$(T_R/\Delta W)^2 - 4C_{D,0}K = 0$$

that is,

$$U_{(T_R)_{\min}} = \left[\frac{2}{\rho}\sqrt{\frac{K}{C_{D,0}}}\frac{\Delta W}{S_{\text{wing}}}\right]^{1/2} \tag{A2}$$

Further, the lift-to-drag ratio derived from Eq. (A1) is

$$\frac{L}{D} = \left[\frac{C_{D,0}}{(2/\rho U^2)(\Delta W/S_{\text{wing}}) + R_F C_{L_{\text{ship}}}} + \frac{2K}{\rho U^2}\left(\frac{\Delta W}{S_{\text{wing}}}\right)\left(\frac{\Delta W}{W}\right)\right]^{-1} \tag{A3}$$

II. Power Required for Level Flight

The power required for steady level flight is

$$P_R = \sqrt{2W^3 C_D^2/\rho S_{\text{wing}} C_L^3}, \qquad P_R \propto \left(C_L^{3/2}/C_D\right)^{-1}$$

Hence, the minimum power required for the aeroship is achieved by maximizing $C_L^{3/2}/C_D$ with respect to C_L. A relation at $(C_D^{3/2}/C_D)_{\max}$ is

$$C_{D,0} = (KC_L/3 + KR_F C_{L_{\text{ship}}})(C_L - R_F C_{L_{\text{ship}}})$$

A solution to this equation gives

$$C_L = \sqrt{3C_{D,0}/K + 4R_F^2 C_{L_{\text{ship}}}^2} - R_F C_{L_{\text{ship}}}$$

The minimum power required can be obtained from these relations. Calculations are needed to compare the value of $C_L^{3/2}/C_D$ for the aeroship and aircraft.

For level flight in which $W = L = \rho U^2 S_{\text{wing}} C_L/2$, a symbolic expression for the cruising velocity is

$$U_{(C_L^{3/2}/C_D)_{\max}} = \left[\frac{2}{\rho}\left(\frac{W}{S_{\text{wing}}}\right)\frac{1}{\sqrt{3C_{D,0}/K + 4R_F^2 C_{L_{\text{ship}}}^2} - R_F C_{L_{\text{ship}}}}\right]^{1/2} \tag{A4}$$

Equation (A4) is symbolic because the parameter

$$R_F = gV_{\text{ship}}/(U^2 S_{\text{wing}}/2)$$

depends on the velocity U. Therefore,

$$U_{(C_L^{3/2}/C_D)_{\max}}$$

is determined by an iteration scheme, and then it is used to evaluate the minimum power required. Nevertheless, the effect of the buoyancy force on the cruising velocity is evident in Eq. (A4). The additional lift and drag due to the presence of the airship module leads to a lower cruising velocity than with aircraft with the same wing and total weight. Similar to conventional airship, the aeroship with a lower cruising speed will be susceptible to strong winds, which is a shortcoming of an aeroship.

III. Climb

As shown in Fig. 2b, the equations of motion for the climb of an aeroship are

$$T - (D_{\text{ship}} + D_{\text{wing}}) - W\sin\theta + L_{\text{ship}}\sin\theta = 0$$

and

$$L_{\text{wing}} + L_{\text{ship}}\cos\theta - W\cos\theta = 0$$

where θ is the climb angle. Substitution of the expression for the drag into the rate of climb

$$R/C = [T - (D_{\text{ship}} + D_{\text{wing}})]U/\Delta W$$

yields

$$R/C = U\sin\theta = U\left[\left(\frac{T}{S_{\text{wing}}} - \frac{\rho U^2}{2}C_{D,0}\right)\left(\frac{\Delta W}{S_{\text{wing}}}\right)^{-1} - \frac{2K\cos^2\theta}{\rho U^2}\left(\frac{\Delta W}{S_{\text{wing}}}\right)\right] \tag{A5}$$

The general behavior is that R/C increases as the relative wing loading decreases. For a propeller-driven aeroship, the thrust available is $T_A = \eta_{\text{pr}}P/U$, where the effective power $\eta_{\text{pr}}P$ can be approximately considered as a constant, and η_{pr} is the propeller efficiency. Therefore, the climb angle is explicitly given by

$$\sin\theta = \left(\frac{\eta_{\text{pr}}P}{S_{\text{wing}}U} - \frac{\rho U^2}{2}C_{D,0}\right)\left(\frac{\Delta W}{S_{\text{wing}}}\right)^{-1} - \frac{2K\cos^2\theta}{\rho U^2}\left(\frac{\Delta W}{S_{\text{wing}}}\right) \tag{A6}$$

An iteration scheme is required for determining the climb angle from Eq. (A6). When the climb angle is not large, under an approximation of $\cos\theta \approx 1$, differentiating Eq. (A6) with respect to U and then setting the result equal to zero, we obtain an approximate solution for the velocity to achieve the maximum climb angle:

$$U_{\theta_{\max}} = \frac{4K}{\rho\eta_{\text{pr}}(P/S_{\text{wing}})}\left(\frac{\Delta W}{S_{\text{wing}}}\right)^2 \tag{A7}$$

Because the power available for a propeller-driven aeroship can be reasonably treated as a constant, the cruising velocity given by Eq. (A4) approximately equals the velocity for the maximum rate of climb: that is,

$$U_{(R/C)_{\max}} \approx U_{(C_L^{3/2}/C_D)_{\max}}$$

where $(R/C)_{\max}$, can be calculated by substituting this approximation into Eq. (A5), and then the climb angle at $(R/C)_{\max}$ can be evaluated by using

$$\sin\theta = (R/C)_{\max}/U_{(R/C)_{\max}}$$

IV. Glide and Stall

The equilibrium between the forces is shown in Fig. 2c. The equations of motion for an aeroship in gliding flight are

$$D_{\text{ship}} + D_{\text{wing}} + L_{\text{ship}}\sin\theta - W\sin\theta = 0$$

and

$$L_{\text{wing}} + L_{\text{ship}}\cos\theta - W\cos\theta = 0$$

where θ is the glide angle. The equilibrium glide angle is then given by $\tan\theta = C_D/C_{L_{\text{wing}}}$, and the decent rate (sink velocity) is

$$U_V = \sqrt{\frac{2}{\rho C_{L_{\text{wing}}}^3/C_D^2}\frac{\Delta W}{S_{\text{wing}}}} \tag{A8}$$

For $(C_L)_{\max}$, the stall velocity of an aeroship is given by

$$U_{\text{stall}} = \sqrt{\frac{2}{\rho[C_{L_{\text{ship}}} R_F + (C_{L_{\text{wing}}})_{\max}]} \frac{W}{S_{\text{wing}}}} \tag{A9}$$

V. Level Turn and Pull-Up Maneuver

The equilibrium between the forces in a level turn is illustrated in Fig. 2d. The motion equations are

$$L_{\text{wing}} \cos\phi + L_{\text{ship}} = W$$

and

$$(W/g)(U^2/R) = L_{\text{wing}} \sin\phi$$

where ϕ is the bank angle and R is the turn radius. The bank angle is given by $\phi = \cos^{-1}(1/n_r)$, where $n_r = L_{\text{wing}}/\Delta W$ is the effective load factor. Based on the motion equations, the turn radius is

$$R = \frac{2q_\infty}{\rho g(\Delta W/W)\sqrt{n_r^2 - 1}} \tag{A10}$$

and the angular velocity $\omega = U/R$, where q_∞ is the dynamic pressure. The expressions for the minimum turn radius and the corresponding velocity are

$$R_{\min} = \frac{4K(\Delta W/S_{\text{wing}})}{\rho g(T/W)\sqrt{1 - 4KC_{D,0}/(T/\Delta W)^2}} \tag{A11}$$

and

$$U_{R_{\min}} = \sqrt{\frac{4K(\Delta W/S_{\text{wing}})}{\rho(T/\Delta W)}} \tag{A12}$$

VI. Takeoff and Landing

The distance s that an aeroship travels along the ground for takeoff is governed by the differential equation

$$\mathrm{d}s = \frac{\mathrm{d}U^2}{2(\mathrm{d}U/\mathrm{d}t)}$$

The acceleration is given by

$$\frac{\mathrm{d}U}{\mathrm{d}t} = \frac{g}{W}[T - D - \mu_r(\Delta W - L_{\text{wing}})]$$

where μ_r is the ground-friction coefficient. Integration of the differential equation can give the ground roll. For simplification, assuming that

$$T \gg D + \mu_r(\Delta W - L_{\text{wing}})$$

we have an estimate

$$s_g \approx \frac{1.21(W/S_{\text{wing}})}{g\rho[C_{L_{\text{ship}}} R_F + (C_{L_{\text{wing}}})_{\max}](T/W)} \tag{A13}$$

For landing, the approach angle is given by $\sin\theta_a = (D - T)/\Delta W$. Similarly, an estimate the ground roll in landing is

$$s_g \approx \frac{1.21(W/S_{\text{wing}})}{g\rho[C_{L_{\text{ship}}} R_F + (C_{L_{\text{wing}}})_{\max}][D/W + \mu_r(1 - L/W)]} \tag{A14}$$

References

[1] Mowforth, E., *A Introduction to the Airship*, No. 3, Airship Association, London, 1991, p. 105.

[2] Khoury, G., "Unconventional Designs, *Airship Technology*, Eds. G. A. Khoury, and J. D. Gillett, Cambridge Univ. Press, Cambridge, England, U.K., 1999, Chap. 15.

[3] Calkins, D. E., "Feasibility Study of a Hybrid Airship Operating in Ground Effect," *Journal of Aircraft*, Vol. 14, No. 8, 1977, pp. 809–815. doi:10.2514/3.58857

[4] Mackrodt, P. A., "Further Studies in the Concept of Delta-Winged Hybrid Airships," *Journal of Aircraft*, Vol. 17, No. 10, 1980, pp. 734–740. doi:10.2514/3.57960

[5] Anders, S., Asbury, S. C., Brentner, K. S., Bushnell, D. M., Glass, C. E., Hodges, W. T., Morris, S. J., and Scott, M. A., "The Personal Aircraft—Status and Issues," NASA TM 109174, Dec. 1994.

[6] Bouras, P., and Fox, T., "An Autonomous Flying Vehicle for Mars Exploration," AIAA Paper 90-3235, Sept. 1990.

[7] Smith, S. C., Hahn, A. S., Johnson, W. R., Kinney, D. J., Pollitt, J. A., and Reuther, J. R., "The Design of the Canyon Flyer: An Airplane for Mars Exploration," AIAA Paper 2000-0514, Jan. 2000.

[8] Levine, J. S., Blaney, D., Connemey, J. E. P., Greeley, R., Head, J., Hoffman, J., et al.,"Science from a Mars Airplane: The Aerial Regional-Scale Environment Survey (ARES) of Mars," AIAA Paper 2003-6576, Sept. 2003.

[9] Guynn, M. D., Groom, M. A., Smith, S. C., Parks, R. W., and Gelhausen, P. A., "Evolution of a Mars Airplane Concept for the ARES Mars Scout Mission," AIAA Paper 2003-6578, 2003.

[10] Young, L. A., Chen, L. A., Aiken, E. W., and Briggs, G. A., "Design Opportunities and Challenges in the Development of Vertical Lift Planetary Aerial Vehicles," *American Helicopter Society Vertical Lift Aircraft Design Conference*, AHS International, Alexandria, VA, Jan. 2000.

[11] Young, L. A., Aiken, E. W., Johnson, J. L., Demblewski, R., Andrews, J., and Klem, J., "New Concepts and Perspectives on Micro-Rotorcraft and Small Autonomous Rotary-Wing Vehicles," AIAA Paper 2002-2816, June 2002.

[12] Corfeld, K. J., Strawn, R. C., and Long, L. N., "Computational Analysis of a Prototype Martian Rotorcraft Experiment," AIAA Paper 2002-2815, 2002.

[13] Young, L. A., Aiken, E. W., Gulick, V., Mancinelli, R., and Briggs, G. A., "Rotorcraft as Mars Scouts," Vol. 1, Inst. of Electrical and Electronics Engineers, Piscataway, NJ, 2002, pp. 1–378.

[14] Kroo, I., "The Mesicopter: A Miniature Rotorcraft Concept," Phase II Report, NASA Inst. for Advanced Concepts, Atlanta, Nov. 2001.

[15] Colozza, A., "Planetary Exploration Using Biomimetics—An Entomopter for Flight on Mars," Phase I Report, NASA Inst. for Advanced Concepts, Rept. NAS5-98051, Atlanta, Oct. 2002.

[16] Colozza, A., "Solid State Aircraft," Phase II Report, NASA Inst. for Advanced Concepts, Rept. NAS5-98051, Atlanta, Nov. 2002.

[17] Pankine, A., "Planetary Science from Directed Aerial Robert Explorers (DARE)," Phase I Report, NASA Inst. for Advanced Concepts, Atlanta, Dec. 2002.

[18] Liu, T., and Liou, W. W., "Aeroship: A New Flight Platform," AIAA Paper 2006-3922, June 2006.

[19] Cheeseman, I., "Aerodynamics," *Airship Technology*, edited byG. A. Khoury, and J. D. Gillett, Cambridge Univ. Press, Cambridge, England, U.K., 1999, Chap. 3.

[20] Anderson, J. D., *Aircraft Performance and Design*, McGraw–Hill, Boston, 1999, Chaps. 5, 6.

[21] Schulte, M., "Iterative Design of the Aeroship through Flight Testing," MS Thesis, Department of Mechanical and Aeronautical Engineering, Western Michigan Univ., Kalamazoo, MI, 2008.

[22] Liu, T., Cattafesta, L., Radezsky, R., and Burner, A. W., "Photogrammetry Applied to Wind Tunnel Testing," *AIAA Journal*, Vol. 38, No. 6, 2000, pp. 964–971. doi:10.2514/2.1079, 2000.

[23] Burner, A. W., Liu, T., and DeLoach, R., "Uncertainty of Videogrammetric Techniques Used for Aerodynamic Testing," AIAA Paper 2002-2794, June 2002.